Comparative Study of the Self-Aggregation of Rhodamine 6G in the Presence of Poly(sodium 4-styrenesulfonate), Poly(N-phenylmaleimide-co-acrylic acid), Poly(styrene-alt-maleic acid)...

ARTICLE *in* THE JOURNAL OF PHYSICAL CHEMISTRY B · SEPTEMBER 2010

Impact Factor: 3.3 · DOI: 10.1021/jp104340k · Source: PubMed

Comparative Study of the Self-Aggregation of Rhodamine 6G in the Presence of Poly(sodium 4-styrenesulfonate), Poly(*N*-phenylmaleimide-*co*-acrylic acid), Poly(styrene-*alt*-maleic acid), and Poly(sodium acrylate)

Ignacio Moreno-Villoslada,*,† Juan Pablo Fuenzalida,† Gustavo Tripailaf,† Rodrigo Araya-Hermosilla,† Guadalupe del C. Pizarro,‡ Oscar Guillermo Marambio,‡ and Hiroyuki Nishide§

Instituto de Química, Facultad de Ciencias, Universidad Austral de Chile, Casilla 567, Valdivia, Chile, Departamento de Química, Facultad Ciencias Naturales, Matemáticas y del Medio Ambiente, Universidad Tecnológica Metropolitana, Santiago, Chile, and Department of Applied Chemistry, School of Science and Engineering, Waseda University, Tokyo 169-8555, Japan

Received: May 12, 2010; Revised Manuscript Received: July 15, 2010

The interaction between rhodamine 6G and different polyelectrolytes is analyzed. Structural aspects differentiate these polyelectrolytes, such as the presence of aromatic groups and the number and localization of their respective charges, which may be directly attached to the aromatic groups or to the polymeric main chain. In the case of poly(sodium acrylate), which does not bear aromatic groups, the polyelectrolyte induces cooperative self-stacking between the dyes which is highly sensitive to the ionic strength, due to the predominance of long-range electrostatic interactions between the polymer and the dye. In the case of poly(sodium 4-styrenesulfonate), whose charge is directly attached to the aromatic groups, a high dispersant ability of the dyes is found and the interaction is less dependent on the ionic strength, due to the predominance of short-range aromatic−aromatic interactions between the dye and the polymer. Among the two polyelectrolytes studied for which the polymeric charge is directly attached to the main chain, and separated from the aromatic group, poly(styrene-*alt*-maleic acid) shows a lower dependence of the interaction on the ionic strength than poly(*N*-phenylmaleimide-*co*-acrylic acid) at a comonomer composition of 1:2, due to a higher linear aromatic density and a lower linear charge density, indicating the importance of hydrophobic forces. Both copolymers exhibit a high ability to induce cooperative self-aggregation of the dye.

1. Introduction

Ionic interactions may be used for the generation of molecular nanostructures, under the so-called ionic self-assembly (ISA) technique.[1] Polyelectrolytes are suitable building blocks that can lead to nanoscale structures by means of their association with complementary charged polyelectrolytes,[2−4] multivalent counterions,[5,6] surfactants,[7−9] or low-molecular-weight molecules susceptible to undergo self-association such as liquid crystals[10] and dyes.[11] To achieve a better control of the structures, ISA takes advantage of secondary interactions such as hydrogen bonding, coordination binding, or aromatic−aromatic interactions, apart from primary long-range electrostatic interactions. Self-assembly of organic nanotube bundles,[12] mechanical extraction of inner shells from multiwalled carbon nanotubes,[13] and controlled flapping motion of molecular flippers[14] have highlighted the utility of harnessing the aromatic−aromatic interactions in designing functional nanomaterials.

Aromatic−aromatic interactions[15−28] take place in the supramolecular assembly of several molecules and play a crucial role in biological systems involving DNA and/or proteins. It is of great interest that both structures and functionalities are determined by the presence of these interactions and are intrinsically related. They are one of the principal noncovalent forces governing molecular recognition and biomolecular structure. They are important in the stabilization of DNA and its association with intercalators.[20,29−31] They also play an important role in protein stabilization[24,25,32,33] and protein functionality, as in enzymes,[26,34] transmembrane channels,[27,28] etc. The main forces driving aromatic−aromatic interactions in water are solvophobic, while site-specific interactions such as dispersion forces, short-range electrostatic interactions, hydrogen bond formation, $\pi-\pi$ interactions, or cation$-\pi$ interactions may also contribute to the free energy and define the geometry of the complexes.[15,35−40] In particular, there has been a significant debate about the role of electrostatic versus dispersion forces on the overall stabilization of aggregates and conformers by aromatic−aromatic interactions.[15,38−40]

ISA is usually accompanied by a cooperative binding mechanism[41,42] so that the molecules bind preferably adjacent to each other: the first bonds stimulate further binding which propagates toward the final self-assembled structures. In particular, charged dye molecules may produce aggregates by self-stacking due to aromatic−aromatic interactions with defined shape and regular mutual overlap interactions. Their interesting luminescent and electronic properties are the basis of the important applications of materials containing this kind of molecules. The cooperative binding of charged dyes on polyelectrolytes is already a classic theme and has been used in polyelectrolyte analytics.[11,42−55] This is the case for porphyrins[11,47−51] and xanthene dyes such as rhodamine B[52] (RB) and methylene blue (MB).[53−55]

* To whom correspondence should be addressed. Fax: 56-63-293520. E-mail: imorenovilloslada@uach.cl.
† Universidad Austral de Chile.
‡ Universidad Tecnológica Metropolitana.
§ Waseda University.

10.1021/jp104340k
Published on Web 08/31/2010

On the other hand, we have recently described that polyelectrolytes containing aromatic rings undergo aromatic−aromatic interactions with aromatic counterions.[52−54,56−63] These interactions have a short-range character, which implies that water molecules of the hydration sphere of the aromatic groups are released when these groups contact each other in aqueous solution. They may constitute the major forces driving the interaction with the counterions. As a consequence of these interactions, we point out as relevant the dispersant ability of polymers such as poly(sodium 4-styrenesulfonate) (PSS) for counterions such as xanthenes dyes,[52−54] or poly(4-vinylpyridine) (P4VP) for counterions such as sulfonated porphyrins,[63] as well as the resistance of the interaction to the cleaving effect of added NaCl. These findings can open new possibilities for the formation of nanostructures under the scope of ISA. By means of these short-range interactions, site-specific binding between the counterion and the polymeric aromatic functional groups is held, and hydrophobic ion pairs are formed; these ion pairs tend to aggregate depending on the polyelectrolyte/counterion ratio, a fact that may be crucial for the behavior, structure, and properties of the systems. Under appropriate conditions the self-stacking tendency of aromatic counterions such as charged dyes may be overcome: in the presence of a moderate excess of polymeric functional groups, ion pairs aggregate, but in the presence of a high excess of the polymer, ion pairs are far from each other and do not aggregate. Thus, these polyelectrolytes may inhibit the cooperative self-binding tendency of the counterions, showing a certain dispersant ability. The dispersant ability of aromatic polyelectrolytes may be of potential use in controlling counterion properties and may serve to monitor the importance of secondary aromatic−aromatic interactions between the polyelectrolyte and the counterions. Changes in the counterion properties, such as luminescent or redox properties,[52,53,61,62] have been described as a consequence of these interactions.

Among the most useful spectroscopic techniques used to analyze aromatic−aromatic interactions, we find ^{1}H NMR.[58,60] Monodimensional spectra may show broadening of the bands and upfield shifting as indicative of the existence of aromatic−aromatic interactions. NOESY experiments may indicate whether the distance between two different molecules is lower than 5 Å. DOSY experiments may serve to monitor the decrease in the diffusion coefficient of the counterions by means of their binding to the polyelectrolyte. In some cases, changes in the UV−vis spectra of the aromatic counterions are found, due to a change in their electronic structure and/or to a change in the environmental conditions due to the short-range interactions.[11,52,53,63] Apart from spectroscopic techniques, separation techniques are also useful to evaluate the binding between molecules. Among these techniques, diafiltration (DF) has emerged as a suitable technique to evaluate the interactions between low-molecular-weight species (LMWS) and polyelectrolytes.[64−71] The main variables managed in DF analyses are the filtration factor (F), defined as the ratio between the volume in the filtrate and the constant volume in the DF cell, the concentration in the filtrate of the LMWS under study ($c_{\mathrm{LMWS}}^{\mathrm{filtrate}}$), the concentration of free LMWS in the cell solution ($c_{\mathrm{LMWS}}^{\mathrm{free}}$), the concentration of LMWS reversibly bound to the polyelectrolyte ($c_{\mathrm{LMWS}}^{\mathrm{rev\text{-}bound}}$), the apparent dissociation constant ($K_{\mathrm{LMWS}}^{\mathrm{diss}}$), defined as the ratio $c_{\mathrm{LMWS}}^{\mathrm{free}}/c_{\mathrm{LMWS}}^{\mathrm{rev\text{-}bound}}$, the DF parameters k^{m}, j, u, and v, and the polymer concentration (mol of monomeric units/L) (c_{P}). The k^{m} and j parameters (the absolute values of the slope of the curve ln $c_{\mathrm{LMWS}}^{\mathrm{filtrate}}$ versus F in the absence and in the presence of the polyelectrolyte, respectively) are related to the strength of the interaction, while v and u are related to the amounts of LMWS reversibly or irreversibly bound to the polymer, respectively. By irreversibly bound, we consider molecules bound in processes that may be reversible with an apparent dissociation constant that tends to zero at the conditions of the experiment.

As mentioned before, PSS and P4VP are found among polyelectrolytes that undergo aromatic−aromatic interactions with aromatic counterions. These polymers have a charged group directly attached to their aromatic benzene side rings. This fact may have an influence on the strength of the interaction forces, as well as on the stabilization of supramolecular structures, since ion pair formation is enhanced by the interaction of the aromatic rings bearing complementary charges. Thus, the localization of the charge and the aromatic group in the polymer may be relevant to the overall interaction observed. To verify this hypothesis, in this paper we will show and quantify the interactions between the positively charged dye rhodamine 6G (R6G) and the following polyanions: PSS, bearing a charged sulfonate group attached to a benzene ring; poly(styrene-*alt*-maleic acid) (P(S-*alt*-MA)), bearing a benzene ring directly attached to the main chain and negatively charged carboxylate groups, also directly attached to the main polymeric chain, but not attached to the aromatic ring; poly(*N*-phenylmaleimide-*co*-acrylic acid) at a comonomer composition of 1:2 (P(PhM_1-*co*-AA_2)), bearing, as well, negative charges and phenyl groups supported in separated parts along the polymer chain; poly(acrylic acid) (PAA), bearing negative charges, but no aromatic rings. See Figure 1 for the molecular structures. R6G aggregation patterns in the presence of these polyelectrolytes will be discussed. ^{1}H NMR, UV−vis spectroscopies (absorbance and emission), and DF have been used.

2. Experimental Section

2.1. Reagents. Commercially available PSS (Aldrich, synthesized from the para-substituted monomer), P(S-*alt*-MA) (Aldrich), PAA (Aldrich), and R6G (Acros) were used to prepare the solutions in deionized distilled water. The synthesis of P(PhM_1-*co*-AA_2) has been described elsewhere.[72] The pH was adjusted with NaOH and HCl. NaCl (Scharlau) was used to adjust the ionic strength in DF experiments. D_2O (Acros, 99.8% D) was used as the solvent for NMR studies.

2.2. Equipment. The unit used for DF studies consisted of a filtration cell (Amicon 8010, 10 mL capacity) with a magnetic stirrer, a regenerated cellulose membrane with a molecular-weight cutoff of 5000 Da (Ultracel PLCC, 25 mm diameter), a reservoir, a selector, and a pressure source. Distilled water was deionized in a Simplicity Millipore deionizer. The pH was controlled on an UltraBasic Denver Instrument pH meter. UV−vis measurements were performed in a Heλios γ spectrophotometer. Fluorescence measurements were made with Perkin-Elmer LS-50B and Sinco FS-2 spectrometers. ^{1}H NMR measurements were made with a JNM-Lambda500 (JEOL, 500 MHz) spectrometer.

2.3. Procedures. Conventional and well-known procedures have been followed for DF, ^{1}H NMR, and UV−vis spectroscopies of absorbance and fluorescence. Particular experimental conditions are provided in the figure captions. Details for DF procedures can be found elsewhere.[69−71] Prior to use, the polyelectrolytes were fractionated over a poly(ether sulfone) membrane with a molecular-weight cutoff of 10 000 Da, and the highest molecular-weight fractions were chosen for DF experiments so that no macromolecule is able to traverse the 5000 Da DF membrane. UV−vis measurements were recorded using optical path lengths ranging between 1.0 and 10^{-2} cm for solutions containing R6G at concentrations between 10^{-6}

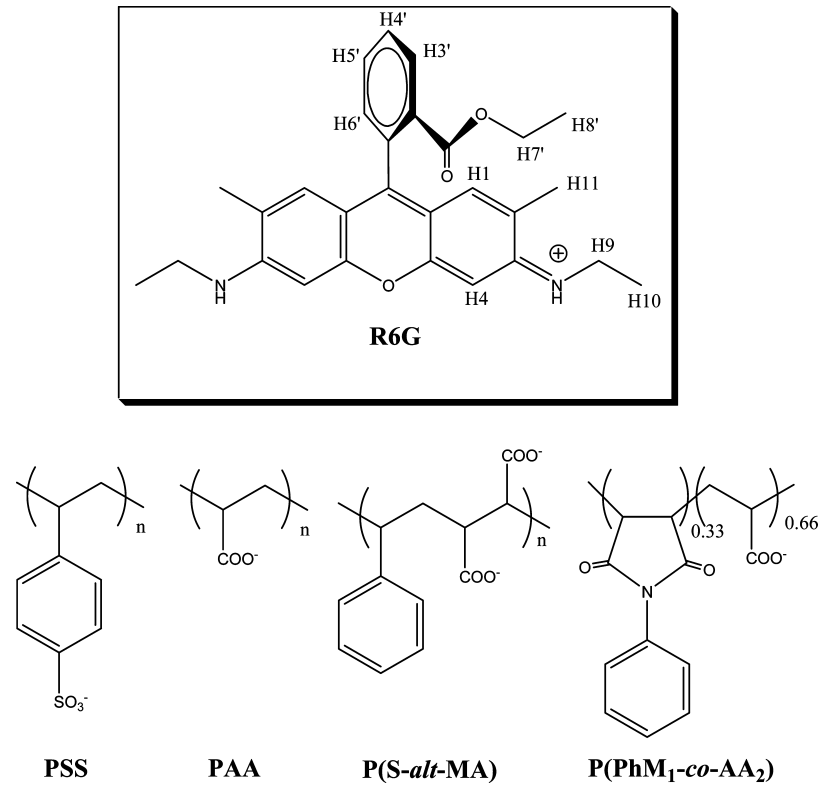

Figure 1. Molecular structures.

and 10^{-3} M to have absorbances in the range of 0.1−1.0. The pH was adjusted to 7 in all experiments. The polymer concentration is given in moles of aromatic (or acrylate in the case of PAA) units per liter in all experiments. Fluorescence measurements were done using a high-pressure xenon arc lamp operating at 775 and 450 V, with excitation and emission slits of 3 or 5 nm. Fluorescence emission was observed at 600 nm for different excitation wavelengths. Fluorescence spectra were obtained after excitation at 440 nm. Solutions of R6G in the presence or in the absence of polyelectrolytes were measured at concentrations of 10^{-6} and 10^{-5} M, depending on the fluorescence intensity. ^{1}H NMR measurements were made in D_2O at 25 °C.

3. Results and Discussion

3.1. R6G Self-Aggregation. Xanthene dyes such as RB[52,73−75] or MB,[53,54,76,77] as well as R6G,[78] undergo self-association at increasing concentrations, forming dimers, trimers, and higher order aggregates. Molecular aggregation of xanthene dyes can drastically modify the absorption characteristics (spectral shifts and band splitting) of the dye. The fluorescent quantum yield and decay time can also be significantly decreased.[79,80] The exciton theory,[81−83] a quantum mechanic method considering the electrostatic interactions between the dipole moments of monomeric units, can be applied to interpret the spectral changes. It predicts a different electronic energy diagram and photophysical behavior of dimers depending on the geometrical distribution of the monomer units. This theory suggests a two-excited-state splitting of the monomer electronic transition for the dimer. The energy gap and the transition probabilities from the ground state to these excited states depend on the relative orientation of the transition moment vectors of the monomeric units in the aggregate. Taking into account the angle between the direction of the dipolar moments and the line linking the molecular centers (θ) and the angle between the transition moments of both monomers in the dimer (α), several specific cases can be considered (see Scheme 1). If $\theta = 90°$ and $\alpha = 0°$, the monomers form the so-called H-type (sandwich-like) dimer, the dipole moments of the monomeric units are aligned in parallel planes, the allowed transition produces a shift of the absorption band to higher energies (H-band), and the dimer does not fluoresce. If $\theta = 0°$ and $\alpha = 0°$, the monomers form the so-called J-type (head-to-tail) dimer, the dipole moments of the monomeric units are aligned coplanar in line, the allowed transition produces a shift of the absorption band to lower energies (J-band), and the dimer fluoresces. Both H- and J-bands will be observed in the absorption spectra for a twisted dimer ($\theta = 90°$ and $\alpha \neq 0$) or for an oblique head-to-tail dimer ($\theta = 0°$ and $\alpha \neq 0$) since transitions to both energy levels are allowed with different probabilities associated: the H-band will be more intense for the twisted sandwich dimer, whereas for the oblique head-to-tail dimer, the J-band should be more intense. Although some of these aggregates can theoretically emit, their relative quantum yield would be much smaller than that of the monomer.

The UV−vis spectrum of R6G presents at least two bands: one, called the monomer band, is centered at 527 nm, while the other, called the dimer band, is centered at 500 nm. At increasing concentrations, the intensity of the dimer band relative to the monomer band increases, as can be seen in Figure 2, revealing the self-association of the dye by means of H-type contacts. At a concentration of 10^{-4} M, dimerization of R6G is readily observed. The addition of other substances to R6G solutions can modify the self-association tendency of the dye. Thus, it can be seen in Figure 2 that the addition of NaCl slightly enhances the self-aggregation of the dye, since the dimer band increases with respect to the monomer band for a given R6G concentration in the presence of the salt.

3.2. Binding of R6G to PAA. Self-aggregation of R6G is nearly negligible at concentrations smaller than 10^{-5} M as can be seen in Figure 2. Typical polyelectrolyte behavior involves

SCHEME 1

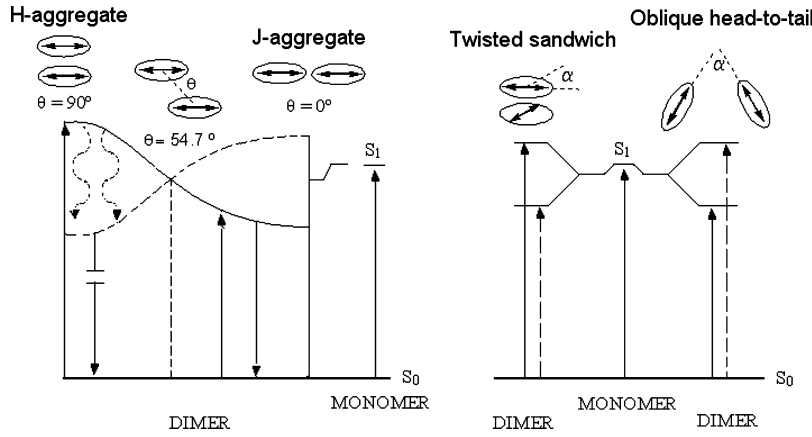

long-range electrostatic interactions with its counterions which are easily cleaved by the addition of electrolytes such as NaCl. The typical polyelectrolyte behavior is clearly illustrated in the study of the interaction between poly(sodium vinylsulfonate) (PVS)[53] or poly(acrylic acid-*co*-maleic acid)[54] and MB or poly(allylamine) (PALA) and anionic porphyrins.[63] A higher local concentration of aromatic counterions around the polyions induces the self-aggregation of the dyes by means of a cooperative binding of the dye on the polymer surface. As MB is a flat molecule, it presents a high tendency to self-aggregate in the presence of PVS and other nonaromatic polyelectrolytes even at very low concentrations of the dye, forming large aggregates that produce a significant shift to higher energies of the UV−vis band due to an extended sandwich-like disposition of the dyes. On the contrary, higher concentrations are needed to induce self-aggregation of RB on PVS,[52] since a benzene carboxylate group perpendicular to the xanthene group may produce steric hindrance to the stabilization of permanent polyaggregates. This seems to be the case for the interaction between PAA and R6G, as inferred from Figure 3. At a dilute concentration of R6G (10^{-5} M) and a 10-fold excess of polymer, the polyelectrolyte partially induces self-aggregation of R6G, producing sandwich-like contacts, as seen by the increase of absorption at higher energies at the expense of the monomer band. The extent of the self-aggregation of the dye around the polyelectrolyte increases as the polymer concentration increases, revealing the cooperative character of the self-binding, as can be seen comparing the R6G spectra in the presence of 10-fold excess PAA (Figure 3a) and 100-fold excess PAA (Figure 3b). Higher order aggregates other than dimers are supposed to be formed since the UV−vis band broadens at higher energies. Note that the R6G monomer band does not shift at these conditions in the presence of PAA. The ratio between the intensities of the band centered at around 500 nm and the one centered at around 527 nm (dimer (D)/monomer (M) ratio) plotted as a function of the polymer concentration in Figure 4 shows the increase in the extent of aggregation by increasing the PAA concentration.

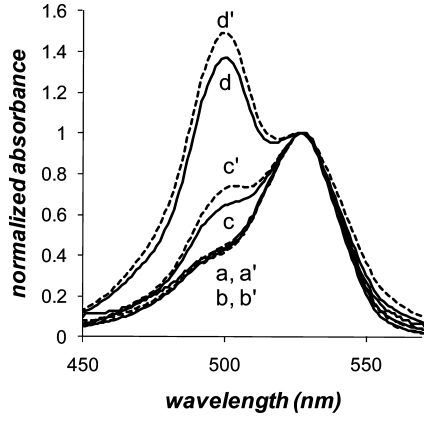

Figure 2. Normalized UV−vis spectra at pH 7 in the absence (a−d) and in the presence (a′−d′) of 0.1 M NaCl of R6G at concentrations of 10^{-6} M (a, a′), 10^{-5} M (b, b′), 10^{-4} M (c, c′), and 10^{-3} M (d, d′).

Since dimers and higher order structures based on H-type contacts are not fluorescent, the differences in the aggregation can be related to fluorescence changes in the solutions. It can be seen in Figure 5 that, as aggregation increases, the fluorescence of the solution decreases. To elucidate whether the emission found is due to monomeric R6G or there is any contribution from aggregates showing a geometrical disposition for the monomers different from the H-type, the emission at 600 nm is plotted as a function of different excitation wavelengths in Figure 6. The plot obtained for pristine R6G has the shape of its absorption spectrum, since the intensity of the emission is proportional to the absorption of the emitting molecules and at this concentration the dye is found in its monomeric form. In the presence of 100-fold excess PAA, the corresponding plot shows broadening to higher energies, indicating a certain contribution of the aggregates to the total fluorescence of the solution. Moreover, the fluorescence spectrum found at these conditions is clearly shifted to higher energies, as can be seen in Figure 7, showing a decrease in the Stokes shift when it is compared with that of the pristine R6G.

At the high R6G concentration needed to perform ^{1}H NMR experiments (10^{-3} M), precipitates appeared even in the presence of a 10-fold excess of the polymer, due to the cooperative binding of the dye on the polymer surface. This effect was also observed for RB in the presence of PVS.[52]

Long-range electrostatic interactions are easily cleaved by the addition of electrolytes such as NaCl, since an excess of the salt screens the interaction. R6G self-aggregation is inhibited in the presence of 0.1 M NaCl, as can be seen in Figure 8. The spectrum of pristine R6G is recuperated in the presence of the salt at both 10- and 100-fold excess of PAA. On the other hand, DF experiments show that in the presence of 0.1 M NaCl and a low excess of PAA (2-fold), the binding of the dye to PAA is nearly negligible, since the rate of filtration is very close to that in the absence of the polymer. The results are shown in Figure 9 and analyzed in Table 1; an apparent dissociation constant that tends to infinity is found for this system.

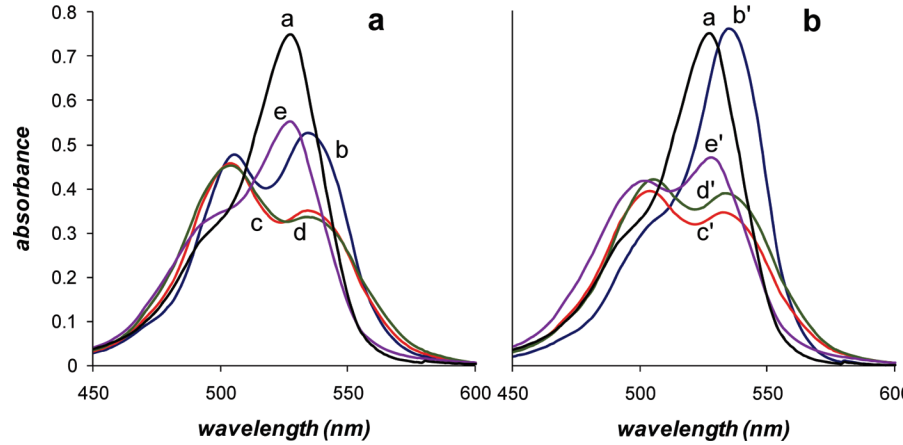

Figure 3. Normalized UV−vis spectra of 1×10^{-5} M R6G solutions at pH 7 in the absence of any polyelectrolyte (a) and in the presence of respectively 1×10^{-4} and 1×10^{-3} M PSS (b, b′), P(PhM$_1$-*co*-AA$_2$) (c, c′), P(S-*alt*-MA) (d, d′), and PAA (e, e′).

3.3. Binding of R6G to PSS. The interaction between the dye and PSS is driven by aromatic−aromatic interactions, as has been demonstrated for other aromatic xanthene counterions such as RB[52,58] or MB.[53] The most important effects found for RB and MB derived from the existence of the short-range aromatic−aromatic interactions are a lower dependence of the interaction on the ionic strength, the formation of ion pairs that tend to aggregate depending on the polymer/aromatic counterion ratio, a high dispersant ability of the dyes in the presence of a large excess of the polymer, the shifting of the UV−vis monomer band to lower energies, and the broadening and upfield shifting of the ^{1}H NMR signals.

Contrarily to PAA, the R6G monomer band is shifted 8 nm to lower energies in the presence of PSS (Figure 3), as was

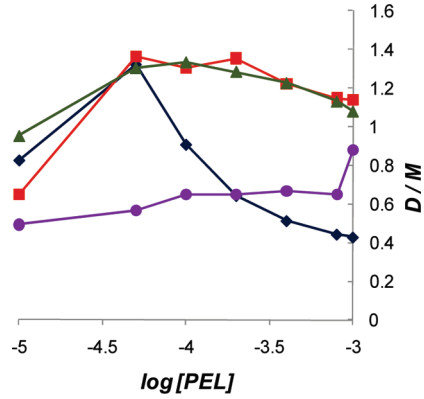

Figure 4. D/M ratio of R6G UV−vis bands as a function of the logarithm of the polyelectrolyte concentration: PSS (◆), P(PhM$_1$-*co*-AA$_2$) (■), P(S-*alt*-MA) (▲), PAA (●).

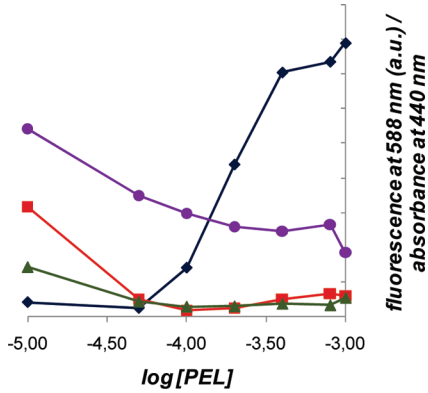

Figure 5. Fluorescence at 588 nm (emission wavelength) versus absorbance at 440 nm (excitation wavelength) as a function of the logarithm of the polyelectrolyte concentration: PSS (◆), P(PhM$_1$-*co*-AA$_2$) (■), P(S-*alt*-MA) (▲), PAA (●).

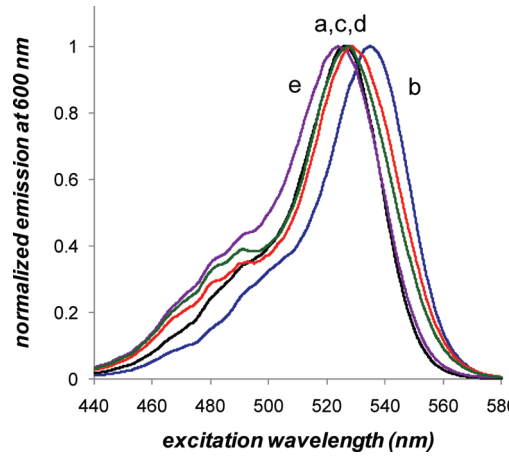

Figure 6. Normalized fluorescence emission at 600 nm and pH 7 as a function of the excitation wavelength of a 10^{-6} M R6G solution in the absence of any polyelectrolyte (a), a 10^{-6} M R6G solution in the presence of 1×10^{-4} M PSS (b), and 10^{-5} M R6G solutions in the presence of 1×10^{-3} M of P(PhM$_1$-*co*-AA$_2$) (c), P(S-*alt*-MA) (d), and PAA (e).

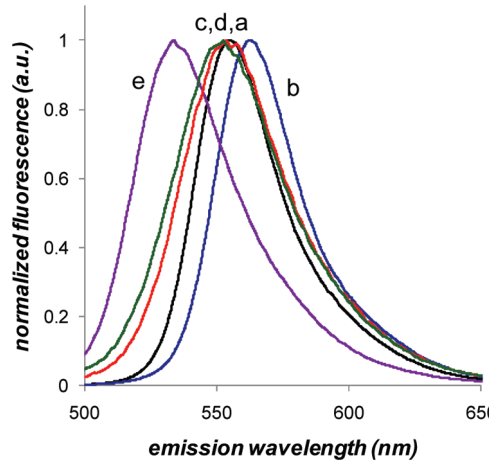

Figure 7. Normalized fluorescence spectra at a 440 nm excitation wavelength and pH 7 of a 10^{-6} M R6G solution in the absence of any polyelectrolyte (a), a 10^{-6} M R6G solution in the presence of 1×10^{-4} M PSS (b), and 10^{-5} M R6G solutions in the presence of 1×10^{-3} M of P(PhM$_1$-*co*-AA$_2$) (c), P(S-*alt*-MA) (d), and PAA (e).

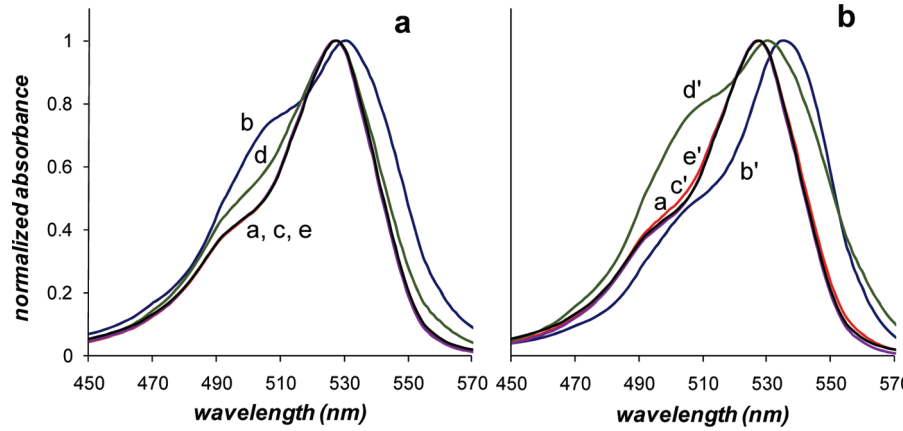

Figure 8. Normalized UV−vis spectra of 1×10^{-4} M R6G solutions in the presence of 0.1 M NaCl at pH 7 in the absence of any polyelectrolyte (a) and in the presence of respectively 1×10^{-3} and 1×10^{-2} M PSS (b, b′), P(PhM_1-*co*-AA_2) (c, c′), P(S-*alt*-MA) (d, d′), and PAA (e, e′).

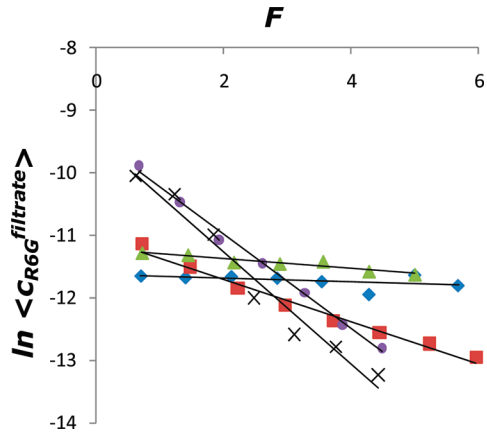

Figure 9. DF profiles of 1×10^{-4} M R6G solutions in the presence of 0.1 M NaCl and at pH 7 in the absence of any polyelectrolyte (×) and in the presence of 2×10^{-4} M of PSS (◆), P(PhM_1-*co*-AA_2) (■), P(S-*alt*-MA) (▲), and PAA (●).

also observed for RB and MB, due to favorable interactions between the transition moment of the dye and the surrounding molecules, a fact that is directly related to the presence of short-range interactions between the dye and the benzenesulfonate groups. The ion pairs produced may be stabilized in a hydrophobic environment. As can be seen in Figure 3a, in the presence of a moderate excess of PSS (10-fold), aggregation of ion pairs is revealed by the intense dimer band showing R6G H-type contacts. On the contrary, in the presence of a large excess of the polymer (100-fold), the dye is randomly distributed on the polymeric binding sites so that ion pairs are far away from each other, preventing their aggregation as can be seen in Figure 3b, where the spectrum of monomeric R6G is found shifted 8 nm. Thus, this polymer exhibits a high dispersant ability of this dye, in contrast to the ability to induce aggregates shown by PAA. Note in Figures 4 and 5 that the dependence of the aggregation of R6G on the polymer concentration takes opposite tendencies comparing PAA and PSS, indicating a different mechanism of interaction. In the case of PSS, the D/M ratio decreases as the polymer exceeds a certain minimum excess (Figure 4) and the fluorescence of the solution increases as the dye disaggregates (Figure 5). The interaction of the dye with the polyelectrolyte does not produce fluorescence quenching, and the corresponding plot in Figure 6 has the shape of the monomer band and is also shifted exactly 8 nm to lower energies with respect to the band corresponding to monomeric free dye. The florescence band is also correspondingly shifted 8 nm to lower energies, as can be seen in Figure 7.

R6G ^{1}H NMR signals broaden and undergo upfield shifting in the presence of PSS as an indication of the existence of aromatic−aromatic interactions, as can be seen in Figure 10. R6G signals corresponding to aromatic protons have been assigned taking RB as a model reference,[58] while signals corresponding to aliphatic protons have been assigned according to their integrates, multiplicity, and chemical shifts. Changes in the polymer bands are also detected for both aromatic and aliphatic protons. Due to the interaction with the dye, the different state of stacking is revealed by an upfield shifting of the polymer band centered around 6.5 ppm, which is assigned to stacked PSS aromatic protons.[54] On the other hand, conformational changes in the polymer associated with ion pair aggregation and/or a more rigid structure may be revealed by a broader distribution of the PSS aliphatic protons.

In the presence of 0.1 M NaCl, ion pair formation and aggregation are still noticeable in the presence of PSS, as can be seen in Figure 8, since short-range aromatic−aromatic interactions are resistant to the cleaving effect of added electrolytes. In the presence of 10-fold excess PSS (Figure 8a), ion pair formation and aggregation are revealed by the shifting of the monomer band and the persistence of the dimer band. In the presence of 100-fold excess PSS, the interaction is not cleaved, as noticed by the recuperation of the monomer band shifted to lower energies; thus, the polymer keeps its dispersant ability. Definite evidence of the resistance to the cleaving effect of added NaCl for the system PSS/R6G is given by DF. As can be seen in Figure 9 and Table 1, the binding of the dye is nearly quantitative and an apparent dissociation constant that tends to zero is found in the presence of 0.1 M NaCl and a low excess of the polymer.

3.4. Binding of R6G to P(PhM_1-*co*-AA_2) and P(S-*alt*-MA). Interesting results are found for the polyelectrolytes P(PhM_1-*co*-AA_2) and P(S-*alt*-MA). A high state of aggregation is found as revealed by the broadening of the UV−vis bands and the high intensity of the band centered at around 500 nm in the presence of both 10-fold and 100-fold excess of the copolymers (see Figure 3). Moreover, ^{1}H NMR signals of the dye disappear in the presence of the copolymers since the low mobility of the molecules associated with the high aggregation state produces fast relaxation times. The ratio between the absorbances at the maxima around 500 and 527 nm (D/M ratio) slightly decreases as the concentration of the polyelectrolytes increases, as can be seen in Figure 4, indicating a low dispersant ability of these polymers. Aggregation of the dye in the presence of an excess of these copolymers produces the quenching of R6G fluores-

TABLE 1: Results for DF of 1×10^{-4} M R6G Solutions in the Presence of 0.1 M NaCl and Different Polyelectrolytes

experiment	c_P (M)	v	u	j	k^m	K_{R6G}^{diss} [a]	linear adjustments for the experimental data[b]	R^2 [b]
R6G−NaCl		0.7	0.3		0.90		$y = -0.90x - 9.46$	0.97
PSS−R6G−NaCl	2×10^{-4}			0.03		$\rightarrow 0$	$y = -0.03x - 11.6$	
P(PhM$_1$-*co*-AA$_2$)−R6G−NaCl	2×10^{-4}	0.5	0.5	0.34		0.53 ± 0.04	$y = -0.34x - 11.0$	0.98
P(S-*alt*-MA)−R6G−NaCl	2×10^{-4}			0.08		$\rightarrow 0$	$y = -0.08x - 11.2$	
PAA−R6G−NaCl	2×10^{-4}	0.9	0.1	0.76		$\rightarrow \infty$	$y = -0.76x - 9.47$	1.00

[a] K_{R6G}^{diss} is calculated following $j/(1-j) \leq K_{R6G}^{diss} \leq k^m j/(k^m - j)$. [b] For linear adjustments, $y = \ln \langle c_{R6G}^{filtrate} \rangle$ and $x = F$. R^2 = linear regression factor.

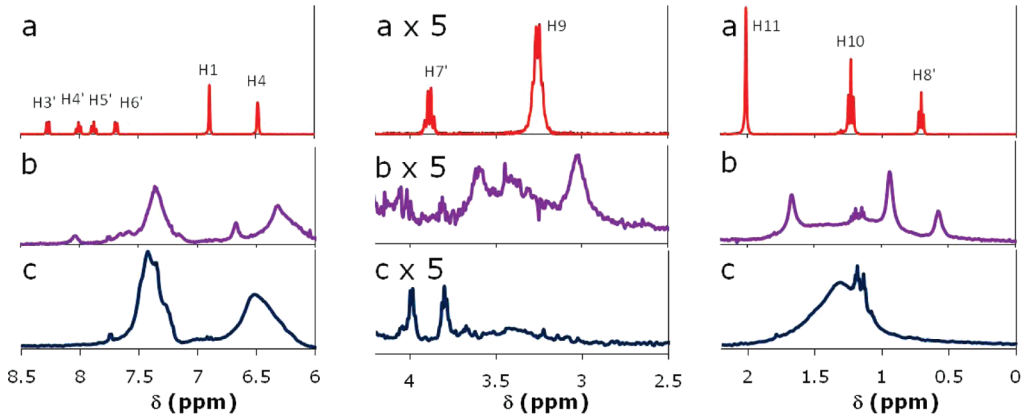

Figure 10. ^{1}H NMR (500 MHz) spectra in D_2O of R6G (10^{-3} M) (a), R6G (10^{-3} M) and PSS (10^{-2} M) (b), and PSS (10^{-2} M) (c).

cence in a wide range of polymer concentration as can be seen in Figure 5. However, the aggregation patterns are different from that in the presence of PAA, as well as the tendency of the D/M ratio at increasing polyelectrolyte concentrations. As a consequence, these polymers do not show a typical polyelectrolyte character as PAA does; neither do they show the dispersant ability of PSS. A different mechanism for the interaction between the dye and these polymers that bear their charge separately from the aromatic group must be postulated.

The broadening of the UV−vis bands to both higher and lower energies may be a consequence of the formation of aggregates showing both H- and J-bands. To elucidate it, their corresponding spectra have been treated by subtracting the contribution of monomeric R6G following the procedures of Arbeloa et al.[84] Taking the spectrum of 10^{-5} M R6G as a reference of pure monomer (M), the molar fraction of the monomer in the presence of the polymers is given by

$$X_{mon} = \frac{A_{500}^{free}/A_{527}^{free}}{A_{500}^{polymer}/A_{527}^{polymer}} \quad (1)$$

where A^{free} and $A^{polymer}$ are the absorbances at the indicated wavelengths in the absence and in the presence of the polymer, respectively. The contribution of aggregated species (Agg) to the total UV−vis spectrum (T) is given by

$$Agg = T - X_{mon}M \quad (2)$$

The corresponding results are shown in Figure 11 and Table 2. Both H- and J-bands are observed with different intensities depending on the polyelectrolyte. As can be read in Table 2, a higher extent of aggregation is found for the copolymers, compared to PAA, since the monomer contribution reaches around 40%, while it reaches 53% for the nonaromatic polyelectrolyte. The spectra of R6G aggregates induced by the

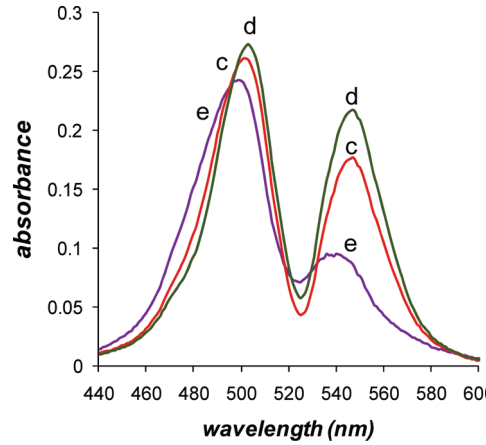

Figure 11. Contribution of aggregates to the total spectrum of R6G (10^{-5} M) in the presence of 10^{-3} M P(PhM$_1$-*co*-AA$_2$) (c), 10^{-3} M P(S-*alt*-MA) (d), and 10^{-3} M PAA (e).

TABLE 2: Calculated Monomer Molar Fraction in 10^{-5} M R6G Solutions in the Presence of a 10^{-3} M Concentration of the Different Polyelectrolytes and Ratio between the Areas Corresponding to H- and J-Bands (H/J)

polymer	X_{mon}	H/J
P(PhM$_1$-*co*-AA$_2$)	0.38	1.6
P(S-*alt*-MA)	0.40	1.3
PAA	0.53	2.4

copolymers present a higher contribution from the J-band relative to the H-band than aggregates formed in the environment of PAA, as can be deduced form their relative areas.

The emission detected for solutions containing R6G and a 100-fold excess of these copolymers may be attributed mainly to free monomers with a minor contribution from aggregates, since the plot of the emission at 600 nm versus the excitation wavelength in Figure 6 shows a shape and a position very similar to those of the one obtained for pristine R6G, but slightly broadened to higher and lower energies. The fluorescence

spectra found at these conditions follow the same pattern, as can be seen in Figure 7.

In the presence of 0.1 M NaCl, the two copolymers exhibit a different behavior. P(PhM_1-*co*-AA_2) is more sensitive than P(S-*alt*-MA) to the cleaving effect of the salt, as can be seen in Figure 8 by the recuperation of the spectra of the pristine R6G at both 10- and 100-fold excess of the polyelectrolyte. On the contrary, P(S-*alt*-MA) still produces aggregation of the dye at these conditions. DF experiments also reveal this different behavior in the presence of added NaCl, as can be seen in Figure 9 and Table 1. While P(S-*alt*-MA) is resistant to the cleaving effect of added NaCl, an apparent dissociation constant of 0.53 for the interaction of the dye with P(PhM_1-*co*-AA_2) is found. The difference found between the two copolymers may be due to the different linear aromatic density in relation to the linear charge density: P(S-*alt*-MA) is an alternate copolymer for which one of the carboxylate units in the maleate residue is protonated at the working pH, while P(PhM_1-*co*-AA_2) contains two acrylate units per aromatic comonomer, showing a lower linear aromatic density, and bears a higher number of carboxylic units dissociated at pH 7, showing a higher linear charge density.

3.5. Different Stacking. The results shown here may highlight some aspects of the features governing the interaction of polyelectrolytes and xanthene dyes such as MB, RB, and R6G. At dilute dye concentrations, these dyes exist in their monomeric form. Typical polyelectrolytes produce a higher concentration of the dyes in their environment due to non-site-specific long-range electrostatic interactions. As a consequence of the higher local concentration, the dyes may cooperatively self-aggregate on the polyelectrolyte surface by means of aromatic−aromatic interactions, mainly forming H-type aggregates. The tendency to form such H-type aggregates depends on the characteristics of the dye, and the planar MB shows a higher tendency than the more voluminous rhodamines. In the case of PAA, aggregates of R6G may adopt a twisted sandwich-like conformation which produces a certain fluorescence as can be deduced by the shift of the maximum of emission at 600 nm to higher excitation energies seen in Figure 6, the shift of the fluorescence spectrum to higher energies shown in Figure 7, and the H/J ratio found in Table 2; according to Fujii et al.,[85] an H/J ratio higher than 1.3 is indicative of twisted sandwich-like dimers.

In the presence of PSS, conditions are given for which the binding of the dyes to the polymeric benzenesulfonate moieties by means of site-specific short-range aromatic−aromatic interactions is more important than the self-stacking tendency of the dyes. This produces the resistance of the dye−polymer interaction to the cleaving effect of added electrolytes and the dispersion of the dyes on the polymeric binding sites. Upon interaction with a 100-fold excess of PSS, the self-stacking of MB, RB, and R6G in the polymer environment is inhibited at a 10^{-5} M concentration of the dyes and their UV−vis spectra are shifted around 8−12 nm to lower energies. The question still remains of whether this shift of the UV−vis band is due to cooperative J-aggregation of the dyes on the polymer domain. However, the J-band for R6G appears at around 545 nm,[83] and the monomer band in the presence of PSS appears at 535 nm. Systems based on porphyrins and polyelectrolytes bearing complementary charged aromatic groups allow distinguishing between J-aggregation by self-stacking and stacking to the polyelectrolyte,[63] since large differences in the position of the respective absorption maxima are found, and the same behavior concerning the ability of such polymers to disperse porphyrins by means of their aromatic−aromatic interaction with the aromatic polymeric groups is found.

On the other hand, the copolymers P(S-*alt*-MA) and P(PhM_1-*co*-AA_2) that bear both aromatic groups and charged groups in separate polymeric segments induce R6G aggregation. These aggregates show a cooperative character since no significant change on the D/M ratio is observed upon increasing the polyelectrolyte concentration. The H/J ratios shown in Table 2 are respectively 1.3 and 1.6, much lower than in the case of PAA. This may indicate the formation of linear aggregates based on twisted sandwich-like contacts. However, the lack of fluorescence found for these aggregates makes us postulate the formation of three-dimensional clusters of the dyes showing both H- and J-bands. As R6G is a rather hydrophobic molecule, these clusters may be included in hydrophobic environments produced by the aromatic rings of the polymers taking into account the charge compensation between the positive charge of the dye and the negative charge of the polymer. The aggregates obtained in the presence of P(S-*alt*-MA) and P(PhM_1-*co*-AA_2) may be stabilized by interactions other than non-site-specific long-range electrostatic interactions, such as hydrophobic forces, short-range electrostatic interactions between the dyes and the carboxylate units, and aromatic−aromatic interactions with the benzene rings stabilized by dispersion forces.

As shown by comparison with the copolymers P(S-*alt*-MA) and P(PhM_1-*co*-AA_2), the presence of a charged group directly bound to the aromatic ring in PSS is fundamental to stabilize the aromatic−aromatic interaction by means of short-range electrostatic interactions between the negative polymeric group and the positive dye. Thus, in this case, the stabilization of the aromatic−aromatic interaction has a high electrostatic component. The hydrophobicity of the polymers is also important for the stabilization of the dye/polymer complex, since copolymers of styrenesulfonate and maleate units showing a lower linear aromatic density exhibit lower binding constants, lower dispersant ability, and lower resistance to the cleaving effect of added NaCl, as has been clearly shown for MB.[54]

Finally, the resistance of these structures to the cleaving effect of added NaCl decreased in the order PSS > P(S-*alt*-MA) > P(PhM_1-*co*-AA_2) > PAA, indicating a decreasing intensity of the short-range components of the interaction. In the case of PSS, as mentioned above, the stabilization of the aromatic−aromatic interactions by short-range electrostatic interactions is pivotal. In the case of P(S-*alt*-MA) and P(PhM_1-*co*-AA_2), the lack of charge complementarity in the polymeric aromatic rings makes the possible short-range interaction weaker. The difference found between P(S-*alt*-MA) and P(PhM_1-*co*-AA_2) may be due to a higher linear aromatic density and a lower linear charge density in the former, which makes the polymer more hydrophobic and possibly more compact. The H/J ratio for the latter is higher, showing a behavior closer to that of PAA. The cleaving of the interaction between R6G and PAA in the presence of the salt corresponds to its typical polyelectrolyte behavior.

4. Conclusions

Different binding patterns have been found between R6G and the polyelectrolytes PAA, PSS, P(S-*alt*-MA), and P(PhM_1-*co*-AA_2). PAA, a polyelectrolyte that does not bear aromatic groups on its structure, shows a typical polyelectrolyte behavior characterized by a high dependence of the interaction on the ionic strength and the ability to induce higher order aggregates of R6G, thus presenting a low dispersant ability of the dye, even in the presence of a 100-fold excess of the polymeric functional groups. This is associated with a long-range electrostatic nature of the interaction between the dye and the

polymer and the presence of short-range aromatic−aromatic interactions between dyes on the polymeric environment that produce cooperative self-stacking. PSS, a polymer bearing aromatic groups and negatively charged sulfonate groups directly attached to them, shows a low dependence of the interaction on the ionic strength and a high dispersant ability of the dye in the presence of an excess of the polymer. This is associated with the predominance of short-range aromatic−aromatic interactions between the dye and the benzenesulfonate polymeric groups. Both P(S-*alt*-MA) and P(PhM_1-*co*-AA_2) have aromatic groups, and their respective negatively charged carboxylate groups are not directly attached to them, but to the main chain. Both polymers show a high ability to induce cooperative self-aggregation of the dye, even in the presence of a 100-fold excess of the polymeric functional groups, probably associated with their hydrophobicity. The aggregates show both H- and J-bands, indicating the formation of twisted sandwich-like aggregates or three-dimensional clusters. The interaction is more sensitive to the ionic strength in the case of P(PhM_1-*co*-AA_1) than in the case of P(S-*alt*-MA) due to a higher linear charge density and a lower linear aromatic density in the former. The differences found in the behavior of R6G in the presence of PSS, P(S-*alt*-MA), and P(PhM_1-*co*-AA_2) reveal that, dealing with oppositely charged polymeric aromatic functional groups and aromatic molecules, stabilization of aromatic−aromatic interactions has a high electrostatic component so that the binding of the benzenesulfonate groups to R6G prevails over the R6G self-stacking, while cooperative self-binding is induced in the presence of uncharged phenyl groups and charged carboxylate groups. The state of aggregation of the dye is determined, however, by the polymer structure as a whole, taking into account the hydrophobicity, charge disposition in the chain, functional groups, conformational properties, linear charge density, and linear aromatic density.

Acknowledgment. We thank Fondecyt (Grant No. 1090341, Chile) and the Global COE program "Practical Chemical Wisdom" at Waseda University from MEXT, Japan, for financial support.

References and Notes

(1) Faul, C. F. J.; Antonietti, M. *Adv. Mater.* **2003**, *15*, 673.
(2) Decher, G. *Science* **1997**, *277*, 1232.
(3) Zhao, Y.; Tanaka, M.; Kinoshita, T.; Higuchi, M.; Tan, T. *Biomacromolecules* **2009**, *8*, 2764.
(4) Park, M.-K.; Onishi, K.; Locklin, J.; Caruso, F.; Advincula, R. *Langmuir* **2003**, *19*, 8550.
(5) Grenha, A.; Seijo, B.; Remuñán-López, C. *Eur. J. Pharm. Sci.* **2005**, *25*, 427.
(6) Willerich, I.; Gröhn, F. *Chem.−Eur. J.* **2008**, *14*, 9112.
(7) Kogej, K.; Evmenenko, G.; Theunissen, E.; Škerjanc, J.; Berghmans, H.; Reynaers, H.; Bras, W. *Macromol. Rapid Commun.* **2000**, *21*, 1226.
(8) Kogej, K.; Evmenenko, G.; Theunissen, E.; Berghmans, H.; Reynaers, H. *Langmuir* **2001**, *17*, 3175.
(9) Antonietti, M.; Conrad, J. *Angew. Chem., Int. Ed. Engl.* **1994**, *33*, 1869.
(10) Thünemann, A. F.; Ruppelt, D.; Ito, S.; Müllen, K. *J. Mater. Chem.* **1999**, *9*, 1055.
(11) Ruthard, C.; Maskos, M.; Kolb, U.; Gröhn, F. *Macromolecules* **2009**, *42*, 830.
(12) Kim, K. S.; Suh, S. B.; Kim, J. C.; Hong, B. H.; Lee, E. C.; Yun, S.; Tarakeshwar, P.; Lee, J. Y.; Kim, Y.; Ihm, H.; Kim, H. G.; Lee, J. W.; Kim, J. K.; Lee, H. M.; Kim, D.; Cui, C.; Youn, S. J.; Chung, H. Y.; Choi, H. S.; Lee, C.-W.; Cho, S. J.; Jeong, S.; Cho, J.-H. *J. Am. Chem. Soc.* **2002**, *124*, 14268.
(13) Hong, B. H.; Small, J. P.; Purewal, M. S.; Mullokandov, A.; Sfeir, M. Y.; Wang, F.; Lee, J. Y.; Heinz, T. F.; Brus, L. E.; Kim, P.; Kim, K. S. *Proc. Natl. Acad. Sci. U.S.A.* **2005**, *102*, 14155.
(14) Kim, H. G.; Lee, C.-W.; Yun, S.; Hong, B. H.; Kim, Y.-O.; Kim, D.; Ihm, H.; Lee, J. W.; Lee, E. C.; Tarakeshwar, P.; Park, S.-M.; Kim, K. S. *Org. Lett.* **2002**, *4*, 3971.
(15) Hunter, C. A.; Sanders, J. K. M. *J. Am. Chem. Soc.* **1990**, *112*, 5525.
(16) Meyer, E. A.; Castellano, R. K.; Diederich, F. *Angew. Chem., Int. Ed.* **2003**, *42*, 1210.
(17) Brunsveld, L.; Folmer, B. J. B.; Meijer, E. W.; Sijbesma, R. P. *Chem. Rev.* **2001**, *101*, 4071.
(18) Tanaka, H.; Litvinchuk, S.; Tran, D.-H.; Bollot, G.; Mareda, J.; Sakai, N.; Matile, S. *J. Am. Chem. Soc.* **2006**, *128*, 16000.
(19) Briseno, A. L.; Miao, Q.; Ling, M.-M.; Reese, C.; Meng, H.; Bao, Z.; Wudl, F. *J. Am. Chem. Soc.* **2006**, *128*, 15576.
(20) Mignon, P.; Loverix, S.; De Proft, F.; Geerlings, P. *J. Phys. Chem. A* **2004**, *108*, 6038.
(21) Lokey, R. S.; Iverson, B. L. *Nature* **1995**, *375*, 303.
(22) Sokolov, A. N.; Friščić, T.; MacGillivray, L. R. *J. Am. Chem. Soc.* **2006**, *128*, 2806.
(23) Mignon, P.; Loverix, S.; Steyaert, J.; Geerlings, P. *Nucleic Acids Res.* **2005**, *33*, 1779.
(24) Tatko, Ch. D.; Waters, M. L. *Protein Sci.* **2003**, *12*, 2443.
(25) Bhattacharyya, R.; Samanta, U.; Chakrabarti, P. *Protein Eng.* **2002**, *15*, 91.
(26) Greenblatt, H. M.; Dvir, H.; Silman, I.; Sussman, J. L. *J. Mol. Neurosci.* **2003**, *20*, 369.
(27) Li, H. L.; Galue, A.; Meadows, L.; Ragsdale, D. S. *Mol. Pharmacol.* **1999**, *55*, 134.
(28) Li, J.; Lester, H. A. *Chem.−Eur. J.* **2005**, *11*, 6525.
(29) Marzilli, L. G.; Pethö, G.; Mengfen, L.; Kim, M. S.; Dixon, D. W. *J. Am. Chem. Soc.* **1992**, *114*, 7575.
(30) McKnight, R. E.; Zhang, J.; Dixon, D. W. *Bioorg. Med. Chem. Lett.* **2004**, *14*, 401.
(31) Martin, J. N.; Muñoz, E. M.; Schwergold, C.; Souard, F.; Asensio, J. L.; Jiménez-Barbero, J.; Cañada, J.; Vicent, C. *J. Am. Chem. Soc.* **2005**, *127*, 9518.
(32) Bodkin, M. J.; Goodfellow, J. M. *Protein Sci.* **1995**, *4*, 603.
(33) Ranganathan, D.; Haridas, V.; Gilardi, R.; Karle, I. L. *J. Am. Chem. Soc.* **1998**, *120*, 10793.
(34) Versées, W.; Loverix, S.; Vandemeulebroucke, A.; Geerlings, P.; Steyaert, J. *J. Mol. Biol.* **2004**, *338*, 1.
(35) Lee, E. C.; Kim, D.; Jurečka, P.; Tarakeshwar, P.; Hobza, P.; Kim, K. S. *J. Phys. Chem. A* **2007**, *111*, 3446.
(36) Kim, E.; Paliwal, S.; Wilcox, C. S. *J. Am. Chem. Soc.* **1998**, *120*, 11192.
(37) Paliwal, S.; Geib, S.; Wilcox, C. S. *J. Am. Chem. Soc.* **1994**, *116*, 4497.
(38) Cockroft, S. L.; Hunter, C. A.; Lawson, K. R.; Perkins, J.; Urch, C. J. *J. Am. Chem. Soc.* **2005**, *127*, 8594.
(39) Cozzi, F.; Annunziata, R.; Benagliz, M.; Cinquini, M.; Raimondi, L.; Baldridge, K. K.; Siegel, J. S. *Org. Biomol. Chem.* **2003**, *1*, 157.
(40) Cozzi, F.; Cinquini, M.; Annunziata, R.; Siegel, J. S. *J. Am. Chem. Soc.* **1993**, *115*, 5330.
(41) Schwartz, G.; Klose, S.; Balthasar, W. *Eur. J. Biochem.* **1970**, *12*, 454.
(42) Faul, C. F. J.; Antonietti, M. *Chem.−Eur. J.* **2002**, *8*, 2764.
(43) Würthner, F.; Thalacker, C.; Diele, S.; Tschierske, C. *Chem.−Eur. J.* **2001**, *7*, 2245.
(44) Imae, T.; Gagel, L.; Tunich, C.; Platz, G.; Iwamoto, T.; Funayama, K. *Langmuir* **1998**, *14*, 2197.
(45) von Berlepsch, H.; Böttcher, C.; Ouart, A.; Burger, C.; Dähne, S.; Kirstein, S. *J. Phys. Chem.* **2000**, *104*, 5255.
(46) Horn, D. *Prog. Colloid Polym. Sci.* **1978**, *65*, 251.
(47) Egawa, Y.; Hayashida, R.; Anzai, J. *Langmuir* **2007**, *23*, 13146.
(48) Kubàt, P.; Lang, K.; Janda, P.; Anzenbacher, P. *Langmuir* **2005**, *21*, 9714.
(49) Lauceri, R.; Campagna, T.; Raudino, A.; Purello, R. *Inorg. Chim. Acta* **2001**, *317*, 282.
(50) Synytsya, A.; Synytsya, A.; Blafková, P.; Ederová, J.; Spěvaček, J.; Slepička, P.; Král, V.; Volka, K. *Biomacromolecules* **2009**, *10*, 1067.
(51) Van Patten, P. G.; Shreve, A. P.; Donohoe, R. J. *J. Phys. Chem. B* **2000**, *104*, 5986.
(52) Moreno-Villoslada, I.; González, F.; Arias, L.; Villatoro, J. M.; Ugarte, R.; Hess, S.; Nishide, H. *Dyes Pigm.* **2009**, *82*, 401.
(53) Moreno-Villoslada, I.; Torres, C.; González, F.; Nishide, H. *Macromol. Chem. Phys.* **2009**, *210*, 1167.
(54) Moreno-Villoslada, I.; Torres-Gallegos, C.; Araya-Hermosilla, R.; Nishide, H. *J. Phys. Chem. B* **2010**, *114*, 4151.
(55) Soedjak, H. S. *Anal. Chem.* **1994**, *66*, 4514.
(56) Moreno-Villoslada, I.; Jofré, M.; Miranda, V.; Chandía, P.; González, R.; Hess, S.; Rivas, B. L.; Elvira, C.; San Román, J.; Shibuhe, T.; Nishide, H. *Polymer* **2006**, *47*, 6496.
(57) Moreno-Villoslada, I.; Jofré, M.; Miranda, V.; González, R.; Sotelo, T.; Hess, S.; Rivas, B. L. *J. Phys. Chem. B* **2006**, *110*, 11809.
(58) Moreno-Villoslada, I.; González, R.; Hess, S.; Rivas, B. L.; Shibuhe, T.; Nishide, H. *J. Phys. Chem. B* **2006**, *110*, 21576.

(59) Moreno-Villoslada, I.; González, F.; Rivas, B. L.; Shibuhe, T.; Nishide, H. *Polymer* **2007**, *48*, 799.
(60) Moreno-Villoslada, I.; González, F.; Rivera, L.; Hess, S.; Rivas, B. L.; Shibuhe, T.; Nishide, H. *J. Phys. Chem. B* **2007**, *111*, 6146.
(61) Moreno-Villoslada, I.; Soto, M.; González, F.; Montero-Silva, F.; Hess, S.; Takemura, I.; Oyaizu, K.; Nishide, H. *J. Phys. Chem. B* **2008**, *112*, 5350.
(62) Moreno-Villoslada, I.; González, F.; Soto, M.; Nishide, H. *J. Phys. Chem. B* **2008**, *112*, 11244.
(63) Moreno-Villoslada, I.; Murakami, T.; Nishide, H. *Biomacromolecules* **2009**, *10*, 3341.
(64) Geckeler, K. E.; Lange, G.; Eberhardt, H.; Bayer, E. *Pure Appl. Chem.* **1980**, *52*, 1883.
(65) Uludag, Y.; Özbelge, H. Ö.; Yilmaz, L. *J. Membr. Sci.* **1997**, *129*, 93.
(66) Vonk, P.; Noordman, R.; Schippers, D.; Tilstra, B.; Wesselingh, H. *J. Membr. Sci.* **1997**, *130*, 249.
(67) Rivas, B. L.; Moreno-Villoslada, I. *J. Phys. Chem. B* **1998**, *102*, 6994.
(68) Rivas, B. L.; Moreno-Villoslada, I. *J. Phys. Chem. B* **1998**, *102*, 11024.
(69) Rivas, B. L.; Pereira, E.; Moreno-Villoslada, I. *Prog. Polym. Sci.* **2003**, *28*, 173.
(70) Moreno-Villoslada, I.; Miranda, V.; Oyarzún, F.; Hess, S.; Luna, M. B.; Rivas, B. L. *J. Chil. Chem. Soc.* **2004**, *49*, 121.
(71) Moreno-Villoslada, I.; Miranda, V.; Chandía, P.; Villatoro, J. M.; Bulnes, J. L.; Cortés, M.; Hess, S.; Rivas, B. L. *J. Membr. Sci.* **2006**, *272*, 137.
(72) Pizarro, G.; del, C.; Marambio, O. G.; Jeria-Orell, M.; Huerta, M.; Rivas, B. L. *J. Appl. Polym. Sci.* **2006**, *99*, 2359.
(73) López Arbeloa, I.; Ruiz Ojeda, P. *Chem. Phys. Lett.* **1982**, *87*, 556.
(74) López Arbeloa, F.; Ruiz Ojeda, P.; López Arbeloa, I. *J. Lumin.* **1989**, *44*, 105.
(75) Mchedlov-Petrossyan, N. O.; Vodolazkaya, N. A.; Doroshenko, A. O. *J. Fluoresc.* **2003**, *13*, 235.
(76) Lewis, G. N.; Goldschmid, O.; Magel, T. T.; Bigeleisen, J. *J. Am. Chem. Soc.* **1943**, *65*, 1150.
(77) Valdés-Aguilera, O.; Neckers, D. C. *Acc. Chem. Res.* **1989**, *22*, 171.
(78) López Arbeloa, F.; Ruiz Ojeda, P.; López Arbeloa, I. *J. Chem. Soc., Faraday Trans.* **1988**, *84*, 1903.
(79) Van der Auweraer, M.; Verschuere, B.; De Schryver, F. C. *Langmuir* **1988**, *4*, 583.
(80) Tsukanova, V.; Lavoie, H.; Harata, A.; Ogawa, T.; Salesse, C. *J. Phys. Chem. B* **2002**, *106*, 4203.
(81) Kasha, M.; Rawls, H. R.; El-Bayoumi, M. A. *Pure Appl. Chem.* **1965**, *11*, 371.
(82) Kemnitz, K.; Tamai, N.; Yamazaki, I.; Nakashima, N.; Yoshihara, K. *J. Phys. Chem.* **1986**, *90*, 5094.
(83) Martínez-Martínez, V.; López-Arbeloa, F.; Bañuelos-Prieto, J.; Arbeloa-López, T.; López-Arbeloa, I. *J. Phys. Chem. B* **2004**, *108*, 20030.
(84) Urrecha-Aguirresacona, I.; López Arbeloa, F.; López Arbeloa, I. *J. Chem. Educ.* **1989**, *66*, 866.
(85) Fujii, T.; Nishikiori, H.; Tamura, T. *Chem. Phys. Lett.* **1995**, *233*, 424.

JP104340K